2024 IEEE/RSJ International Conference on Intelligent Robots and Systems (IROS)
October 14-18, 2024. Abu Dhabi, UAE

External Interaction Estimation of 6-PSS Parallel Robots with Embodied Mechanical Intelligence

Jingyuan Xia, Zecai Lin, Xiaojie Ai, Guangjun Yu* and Anzhu Gao*

Abstract—**Traditional interaction perception of parallel robots relies on a six-dimensional force sensor for contact sensing at their distal end. However, the sensor body occupies the space of moving platform and also increases the load on the robot actuations. To enable both minimization and embodied intelligence, this paper proposes an external interaction estimation method with embodied mechanical intelligence by embedding two single-axis force sensors in each leg of 6-PSS parallel robot. The method uses a backward propagation neural network optimized by sparrow search algorithm, and it can simultaneously estimate the external force and its position using information from multiple single-axis force sensors and the encoder of driving motor. The experimental platform is established to collect the data and train the network. The result shows that the force estimation mean error is 2.4% and the position estimation error is 2.9%. A demonstration with a virtual display interface showing the reconstructed parallel robot pose, and the interaction force and its pose using the proposed estimation method, indicates the effectiveness of the proposed interaction method with embodied mechanical intelligence for 6-PSS parallel robot.**

I. INTRODUCTION

In recent years, robotics technology has undergone rapid development, and robots have been widely used in industry and social life [1-4]. Among them, parallel robots have the advantages of high rigidity, compact structure, good precision kinematic performance and high load-carrying capacity [5, 6]. Currently, there are many practical applications of parallel robots, such as parallel mechanical tools [7], manufacturing [8], and sensing [9, 10]. However, most of the parallel robot lack a way to interact with people and perceive the external environment. The lack of this capability means parallel robots can come across as inflexible, unable to adapt to dynamically changing scenarios. This rigidity limits their functionality and safety, and also diminishes their practical value in fields such as the service industry.

To estimate the force applied to the end of a parallel robot, some studies have been conducted. Some researchers integrate a six-dimensional force sensor at the end of the parallel robot, thus enabling the robot to acquire information about the force and moment [11]. However, there are several problems with this approach. The additional six-dimensional force sensor needs to occupy some workspace at the end of the robot, which will increase the overall size of the parallel robot. Besides, a commercial six-dimensional force sensor is usually expensive, which limits its practical industrial applications. Third, the applied force adds an extra moment due to the arrangement of the sensors, thereby increasing the overall inertia. Another method is to build a model to establish the relationship between the parallel robots' drive, structure and external forces. For example, Black *et al.* proposed a method to estimate the end force of parallel continuum robot using the pose and actuation [12]. Lindenroth *et al.* studied the contact of the entire parallel robot structure and apply a disturbance observer based on generalized torque and motor current measurements to estimate external forces from motor currents and dynamics models [13]. However, such methods have the drawback of low efficiency and accuracy. Additionally, some scholars embedded multiple single-axis force sensors inside the robot for external force estimation. The information from the single-axis force sensors and the structural state of the parallel robot are used to estimate the external forces at the end [14, 15]. Such methods have several advantages. Firstly, the price of single-axis force sensors is relatively low compare to a multi-dimensional force sensor. Furthermore, embedding a single-axis force sensor between the moving platform and static platform does not affect the overall kinematics performance and the stiffness of the robot. For example, Wang *et al.* developed a novel six-axis force/torque sensor that utilizes a parallel structure and featuring full pre-stressing [16]. But their work just considered a static parallel structure and did not account for the condition of the structure changes. Wang *et al.* embedded six single-axis force sensors in a Stewart parallel robot and designed conventional neural networks and physical model-based neural networks to determine the three-axis force at the end of the parallel robot while their work could only calculate the magnitude of the external force and did not include the contact position [17]. To sum up, current methods for measuring interaction force of parallel robots suffer from issue such as occupying workspace or low calculation efficiency accuracy or ignoring contact position.

The contribution of this work is to propose an external interaction estimation method with embodied mechanical intelligence by embedding two single-axis force sensors in each leg of 6-PSS parallel robot. The backward propagation neural network optimized by sparrow search algorithm is used to estimate the external force and its position using the information from multiple single-axis force sensors and the

This work was supported in part by the National Natural Science Foundation of China (62373248); the Shanghai Rising-Star Program (22QC1401400); the Science and Technology Commission of Shanghai Municipality (22511101602, 20DZ2220400). (Corresponding author: Guangjun Yu and Anzhu Gao).

Jingyuan Xia. Zecai Lin, Xiaojie Ai and Anzhu Gao are with the Institute of Medical Robotics and Department of Automation, Shanghai Jiao Tong University, and the Key Laboratory of System Control and Information Processing, Ministry of Education, Shanghai 200240, P. R. China.

Guangjun Yu is with the Second Affiliated Hospital, The Chinese University of Hong Kong, Shenzhen, Guangdong, 518172, P.R. China

pose of the parallel robot. The experimental results show that the errors of estimation in contact position and force are 2.9% and 2.4%, respectively. The rest of this paper is organized as follows. Section II introduces the structure design and sensors configuration of parallel robot; Section III presents the SSA-BP neural network-based external force estimation methods, Section IV conducts the experiments to validate the effectiveness of the proposed method and analyzes the experimental results. Section V makes the conclusion.

II. Structure Design with Embodied Mechanical Intelligence

The mechanical model of the robot and its mechanism schematic are shown in Fig. 1. The parallel robot employs a conventional 6-PSS parallel robot structure. Six spherical-hinge joints $A_1, A_2, A_3, A_4, A_5, A_6$ are fixed on the moving platform and six corresponding spherical-hinge joints $B_1, B_2, B_3, B_4, B_5, B_6$ are fixed on the static platform. Each pair of spherical hinges is connected by a rod. During assembly, parts must be tightened to prevent loosening. On the static platform, servo motors drive the gears to control the linear modules, which in turn cause the six spherical hinges to move horizontally along symmetrically distributed tracks, thereby driving the movement of the moving platform. This structure provides excellent stability and rigidity. To calculate the pose and control the parallel robot, the kinematic model of the parallel robot can be established according to the relevant literature [18].

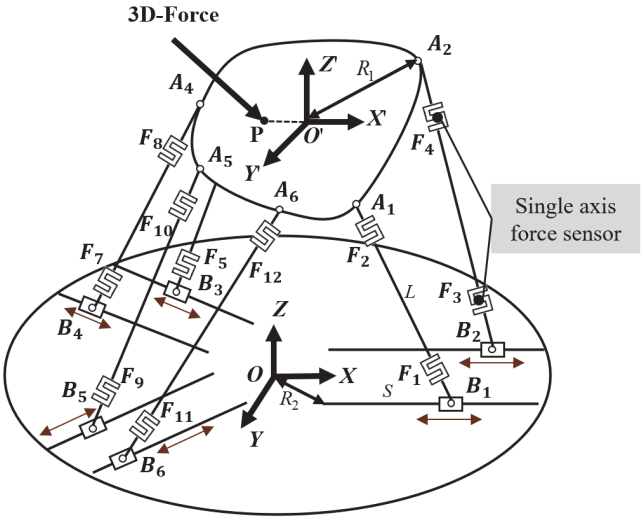

Fig. 1. Structure design of the developed 6-PSS parallel robot with two single-axis force sensors embedded in each line.

As shown in Fig. 2, when an external force is applied to the moving platform of the parallel robot, the embedded force sensors provide real-time feedback. The values from the force sensors and the readings from the motor encoders are used as inputs. Through the processing of a machine learning algorithm, the current force magnitude and contact position of the platform can be obtained as outputs. In this way, parallel robots achieve interaction and sensing capabilities without occupying additional space on the moving platform. The detailed design of this neural network will be introduced in Section III. Two single-axis force sensors are fixed on each connecting leg to collect the axial force information. There are two advantages to this sensor arrangement. One is to determine whether the legs of the parallel robot are subjected to external forces. This is because the difference between the two sensors on the same leg is equal to the gravitational force along the axial direction of the rod.

$$P_2 - P_1 = G \cdot \cos(\theta) \tag{1}$$

where P_2 is the upper force transducer value, P_1 is the lower force transducer value, and θ is the angle of inclination of this axis relative to the static platform. When the values of the two sensors of a rod deviate from the equilibrium equation, it is considered that the force on this leg is abnormal, which indicates that the force on this leg is anomalous. The second benefit is to ensure the uniqueness of the solution of the network. Since there are multiple solutions to the forward kinematics of parallel robots, the difference between the two sensors on a leg is related to the current orientation of the leg.

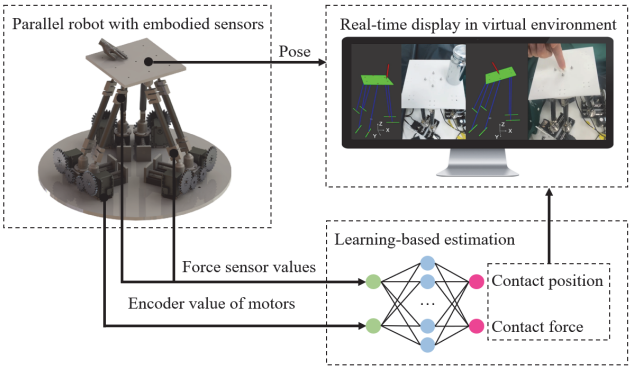

Fig. 2. The concept of embodied mechanical intelligence of 6-PSS parallel robot for external interaction estimation.

III. Interaction Estimation Method

In this section, the neural network optimized by the sparrow search algorithm used to estimate the end force magnitude and position will be introduced.

A. Framework of Neural Network

As the goal of this paper is to estimate the magnitude and contact position of the end external force. The estimation is divided into two distinct tasks, and two parallel networks are constructed to finish these tasks, respectively. One of the networks is dedicated to estimating the force magnitude and the other to estimate the force position. First the data was preprocessed for normalization according to the Eq. (2).

$$X_{norm} = \frac{x - x_{\min}}{x_{\max} - x_{\min}} \tag{2}$$

where $x_{\max}$ and $x_{\min}$ are the vectors consisting of the maximum and minimum values of each feature of the sample. Regarding the estimation of force magnitude, we approach it as a regression problem. The BP neural network a feed-forward neural network which is trained by a back-propagation algorithm. Here, it is employed for this estimation task, and the mean square error is chosen as the

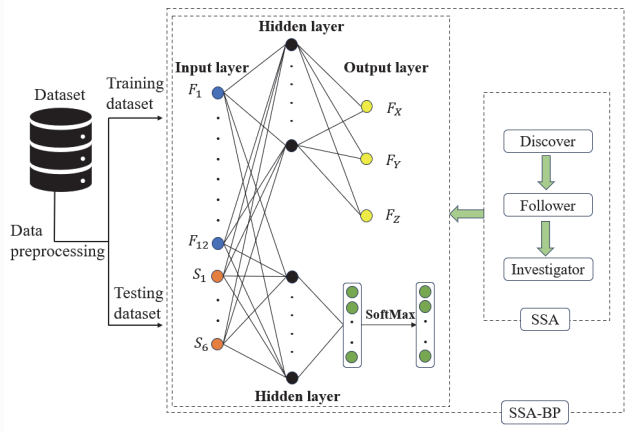

Fig. 3. Framework of estimation method. Two parallel networks are trained to estimate the magnitude and position of the force and their parameters are optimized by sparrow search algorithm.

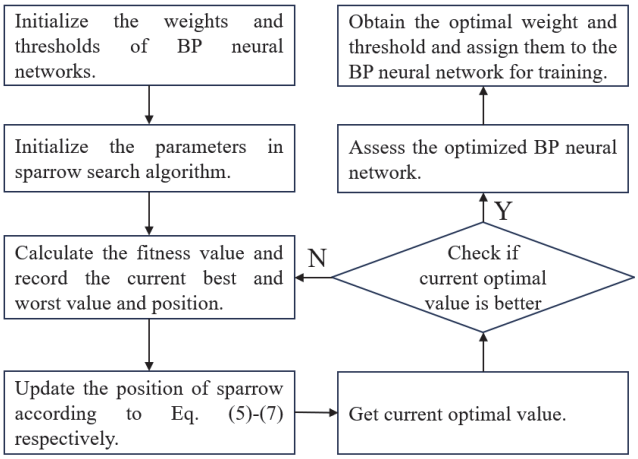

Fig. 4. The process of the sparrow search algorithm to optimize the BP neural network.

loss function to measure the accuracy of estimations. The loss function is defined in Eq. (3). The number of hidden layers is one and the activation function is the ReLu function.

$$Loss_F = \frac{1}{n} \times \sum_{i=1}^{n} \left(y_i^* - y_i \right)^2 \tag{3}$$

where y_i^* and y_i is the ground truth and predictive value of the force. On the other hand, the estimation of force position is treated as a classification problem. This paper represents the contact as nine discrete points arranged in a 3×3 grid on the moving platform. The distance between adjacent points is 50 mm. The problem of estimating the position thus becomes to determine which of these nine positions the point of contact belongs to.

Since the contact position in this study is discretized into nine points, we adopt one-hot encoding for these points. BP neural network is utilized for estimation, and a Softmax layer is added to the final output layer to transform the outputs into a probability distribution. The cross-entropy loss function is chosen as the loss function for this task during the training process. The loss function is defined in Eq. (4). The hidden layer is one layer and the activation function is the ReLu function.

$$Loss_p = -\frac{1}{n} \sum_{i=1}^{n} \sum_{c=1}^{9} y_{ic} \, log\left(P_{ic} \right) \tag{4}$$

where y_{ic} is a sign function, if i is a true category, $y_{ic} = 1$, otherwise, $y_{ic} = 0$. p_{ic} is the estimated probability that the model is c for the sample of class i.

B. *Network Optimized by Sparrow Search Algorithm*

Sparrow search is an optimization algorithm which was proposed in 2021 [19, 20]. Sparrow search algorithm consists of three parts: discoverer, follower, and investigator.

The process for the updated iteration is as follows: The position of the discoverer is updated according to the following factors:

$$X_{k,l}^{t+1} = \begin{cases} X_{k,l}^{t} \exp\left(-\dfrac{k}{a \times \lambda_{\max}} \right), & R_2 < S \\ X_{k,l}^{t} + QL, & R_2 \geq S \end{cases} \tag{5}$$

where $X_{k,l}^{t}$ is the maximum dimension value of the k^{th} sparrow at the t^{th} iteration. $\lambda_{\max}$ is the maximum number of iterations. R_2 and S are warning and safety thresholds. Q is a random number obeying a normal distribution. L is an identity matrix of $1 \times d$, d is number of variables. α is a random value $\in [0,1]$. The position of the follower is updated according to the following factors:

$$X_{k,l}^{t+1} = \begin{cases} Q \exp\left(-\dfrac{X_w^t - X_{k,l}^t}{k^2} \right), & k > \dfrac{n}{2} \\ X_p^t + \left| X_{k,l}^t - X_p^{t+1} \right| A^T \left(AA^T \right)^{-1} L, otherwise \end{cases} \tag{6}$$

Here, X_w^t is the current global worst position at the t^{th} iteration. X_p^t represents the optimal position value at iteration t, and A is a $1 \times d$ matrix where each element has the value -1 or 1. During each iteration, the investigators' position is updated according to following factors:

$$X_{k,l}^{t+1} = \begin{cases} X_b^t + \mu \left| X_{k,l}^t - X_b^t \right|, & f_k > f_b \\ X_{k,l}^t + \tau \left(\dfrac{\left| X_{k,l}^t - X_w^t \right|}{\left(f_k - f_b \right) + \varepsilon} \right), & f_k = f_b \end{cases} \tag{7}$$

where X_b^t represents the current global best position value at the time of iteration, μ is a random number obeying a normal distribution, τ is a random number distributed in [-1,1]. In the optimization process of sparrow search algorithm, the fitness function is loss of the training set and the execution process of algorithm of SSA-BP neural network is shown in Fig. 4.

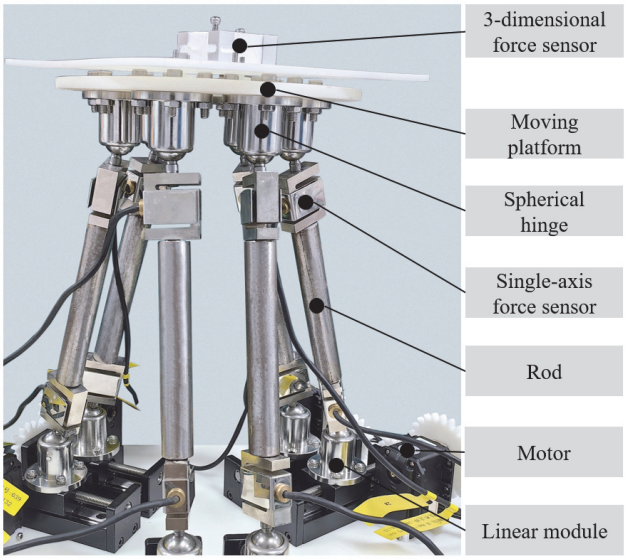

Fig. 5. Experimental platform. The platform includes the embodied sensing parallel robot, digital transmitter and a three-dimensional force sensor.

Table 1. Parameters of 6-PSS parallel robot.

Parameter	Value
Radius of the moving platform R_1	44 mm
Spherical hinge angle distribution	±27°, ±92°, ±147°
Radius of the moving platform R_2	60 mm
Orbit angle distribution of linear modules	-120°, 0°, 120°
Length of linear modules S	53 mm
Rod length L	188 mm

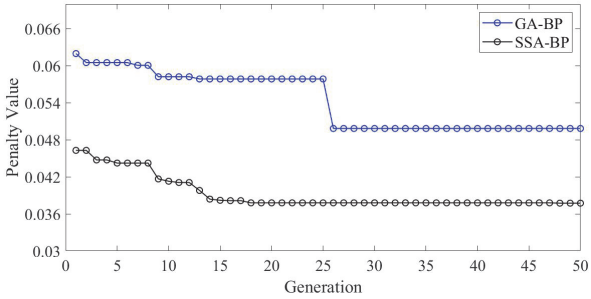

Fig. 6. Comparison between iterative evolution curves of SSA-BP and GA-BP. The number of generations for optimization is 50.

IV. Experiment and Results

A. Experimental Setup

The prototype and parameters of the parallel robot are shown in Fig. 5 and Table. 1. The driving motors of the parallel robot are servo motors (MX-28AR, Dynamixel, Robotics, South Korea). The accuracy of the linear modules is 0.1 mm (Haijie Technology Co., Ltd.). The single-axis force sensors (Qisheng Sensing Co., Ltd., China) have a range of ±30 N and a resolution of 1 mN. These sensors are connected to a personal computer (PC) via a digital transmitter using RS485 communication. The three-dimensional force sensor (Hefei Force Only Sensor Co., Ltd., China) has an X/Y-direction range of ±20 N with an accuracy of 1 mN, and a Z-direction range of ±30 N with an accuracy of 1 mN, which is used to obtain the ground truth. The three-dimensional force sensor is also connected to the PC via a digital transmitter using RS485 communication.

B. Results and Analysis

To collect data from the parallel robot in various poses, we control the parallel robot move to different poses respectively and fix the three-dimensional force sensors at nine points sequentially. Then three-dimensional force is exerted to the sensors without eccentricity. In addition, the parallel robots move along each direction separately at low speeds and force is applied on the moving platform to obtain the data when the parallel robot is moving. After 20000 sets of data were collected, we divided the training and testing sets in the ratio of 4:1 and trained them with the above algorithm. For position estimation problem, we chose a sample of data where the external forces were greater than 0.8 N because it is difficult to estimate the position when the force is too small. The collected data was validated by the above algorithm.

The force magnitude estimation problem was studied first. During the training process, the parameters of the sparrow algorithm were initialized as follows: the size of the sparrow population was set as 30, the maximum number of iterations $\lambda_{\max}$ was set as 50, the safety value S was set as 0.6, the proportion of discoverers was set as 0.7, the proportion of sparrows aware of danger R_2 was set as 0.2. The parameters of back propagation neural network were set as follows: the number of training epochs was set as 150, the number of hidden layer nodes was 36, the learning rate was 0.001 and batch size was 32. In Fig. 6, with the iterative evolution, the RMS error of estimated external force on testing set declined

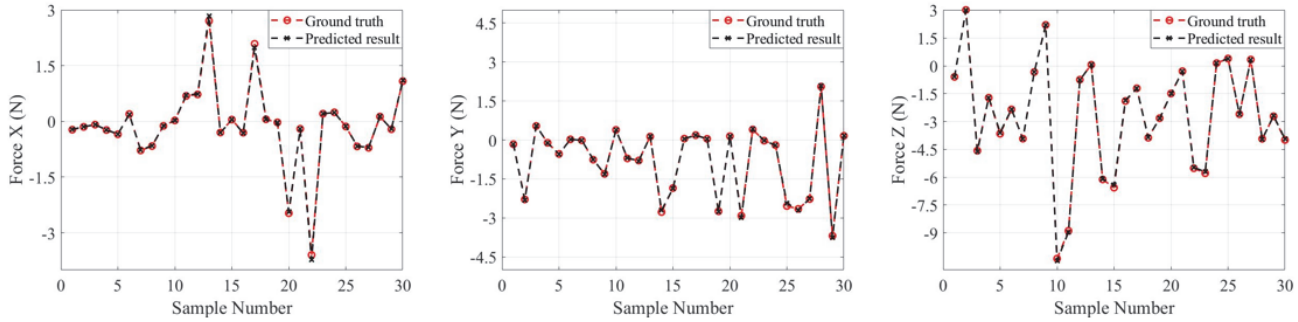

Fig. 7. Samples' ground truth and estimated values of the force along x, y and z direction on the testing set.

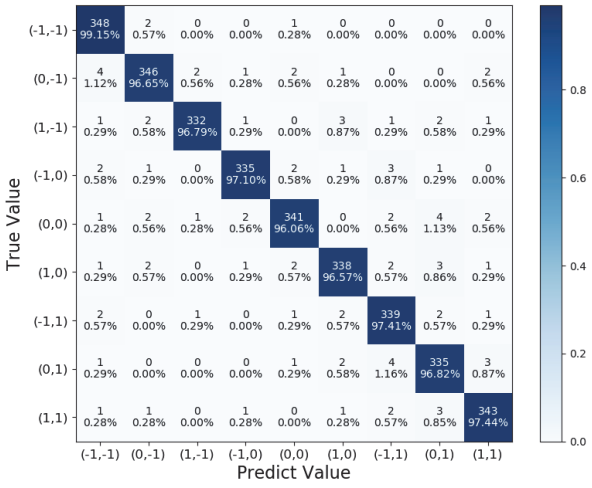

Fig. 8. Distribution of force position prediction accuracy

effectively. Results show that results of sparrow search algorithm are better than genetic algorithm. Fig. 7 shows the results of some sample estimation on the testing set, where the mean error of force magnitudes is 2.4% on the testing set.

To estimate the contact position of the force. The size of the sparrow population was set as 30, the maximum number of iterations $\lambda_{\max}$ was set as 50, the safety value S was set as 0.6, the proportion of discoverers was set as 0.7, the proportion of sparrows aware of danger R_2 was set as 0.2, the number of training epochs was 150, the number of hidden layer nodes was 36, the learning rate was 0.001 and batch size was 32. For the problem of force position estimation, BP-Softmax neural network, radial basis function neural network and SVM classification model were used as a comparison. Among them, the accuracy of SSA-BP-Softmax neural network for classification on the testing set was 97.1% and the accuracy of BP-Softmax neural network, radial basis function neural network and SVM classification are 92.1%, 87.3% and 93.4% respectively. Fig. 8 illustrates the estimation accuracy and error for different external force points. For those misjudged points, they often had a very small force in the z-direction. At this time, the direction of the force is parallel to the moving platform. Since the moment is not changed when the force moves along its line of action, the point of application of the force moving along the line of action still falls on this plane, which may cause misjudgment. When the force in the Z direction is slightly larger, the contact position prediction becomes accurate.

To gain the real-time visualization of force magnitudes and position on the moving platform, we developed a virtual environment tailored for the ROS platform using Rviz. The current pose of the 6-PSS parallel robots was calculated by forward kinematics based on the six encoder values obtained from the servo motors. Within this virtual realm, we presented the estimated force positions and magnitudes in real-time, offering a comprehensive understanding of the robot's dynamic interactions. In Fig. 9, we allowed the parallel robot to move along the Z-direction. During the movement, the system could well estimate the magnitude of the external force and the position of the force. The payload of Fig. 9(a) and (b) were 600 g at different applied position with different Z-direction movements; the payload of Fig. 9(c) and (d) were 300 g at the same applied position with different Z-direction movements. In Fig. 10, we controlled the parallel robot move to different poses. Then an external force was applied by hand to different positions on the moving platform. Fig. 10(a) and (b) show the estimated external force with different applied position when the position of the moving platform pose was different, Fig. 10(c) and (d) show the estimated external force with different applied position when the orientation of the moving platform pose was different.

V. CONCLUSION

This paper has proposed an external interaction estimation method that incorporates embodied mechanical intelligence by integrating two single-axis force sensors into each leg of the 6-PSS parallel robot. The experimental results have shown that the mean error of contact position estimation and force magnitude estimation is 2.9% and 2.4%, respectively. The proposed estimation method of external interaction enables both minimization and embodied intelligence. A demonstration with a virtual display interface showing the reconstructed parallel robot pose, and the interaction force and its pose using the proposed estimation method is established.

In future, considering that the used dataset is relatively small, it is feasible to use data enhancement methods to obtain

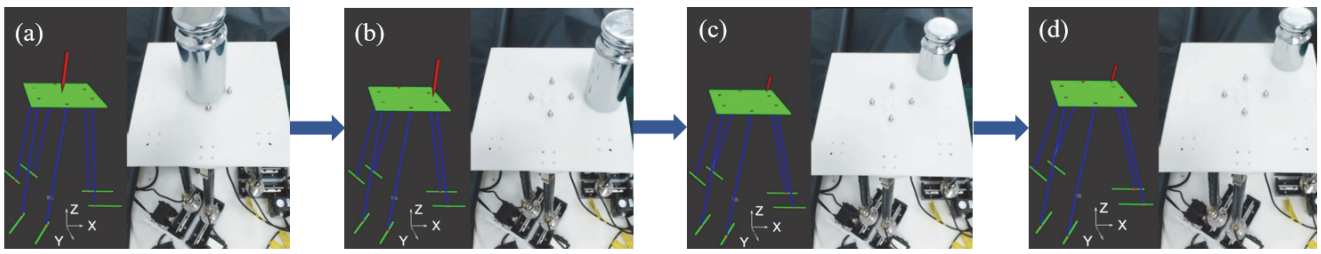

Fig. 9. Force and position estimation of the developed parallel robot with different payloads and Z-direction robot motion. The payload of (a) and (b) were 600 g at different applied position with different Z-direction movements; the payload of (c) and (d) were 300 g at same applied position with different Z-direction movements.

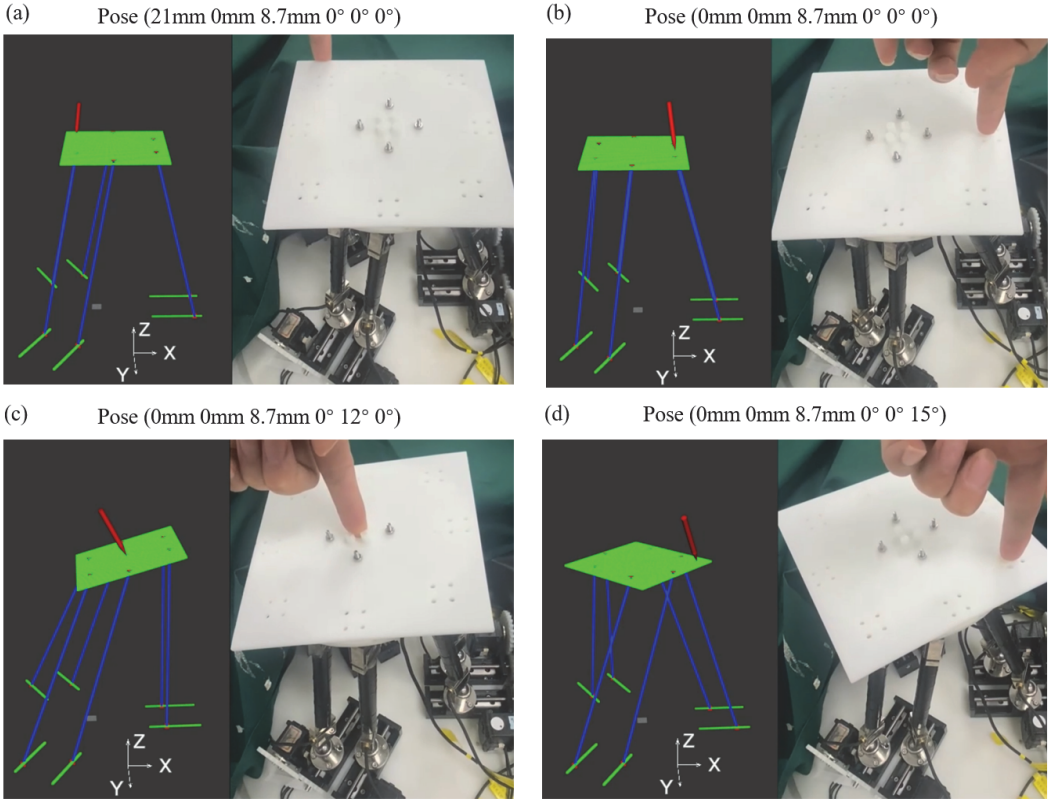

Fig. 10. Force and position estimation of the developed parallel robot with different payloads and variable robot motions. (a) and (b) showed the estimated external force with variable applied position under the same orientation, (c) and (d) showed the estimated external force with variable applied position under the same position.

more data. For example, some generative neural network such as GAN can be used to get diverse data to help generalized the model. Besides, it is expected to conduct admittance control or impedance control for the parallel robot using the estimated external force, thus ensuring the safe interaction between the parallel robot and the surroundings.

REFERENCE

[1] A. Gao *et al*., "Progress in Robotics for Combating Infectious Diseases," *Science Robotics*, vol. 6, no. 52, 2021, Art. no. eabf1462

[2] F. Sherwani *et al*., "Collaborative Robots and Industrial Revolution 4.0 (IR 4.0)," *2020 International Conference on Emerging Trends in Smart Technologies (ICETST)*, Karachi, Pakistan, 2020, pp. 1-5

[3] Y. Shen *et al*., "Robots Under COVID-19 Pandemic: A Comprehensive Survey," in *IEEE Access*, vol. 9, pp. 1590-1615, 2021

[4] R. S. Peres *et al*., "Industrial Artificial Intelligence in Industry 4.0 - Systematic Review, Challenges and Outlook," in *IEEE Access*, vol. 8, pp. 220121-220139, 2020

[5] P. Etienne, et al. "Pulleys and Force Sensors Influence on Payload Estimation of Cable-driven Parallel Robots." *2018 IEEE/RSJ International Conference on Intelligent Robots and Systems (IROS)*. IEEE, pp. 1429-1036, 2018

[6] J. Meng *et al*., "A Geometric Theory for Analysis and Synthesis of Sub-6 Dof Parallel Manipulators," in *IEEE Transactions on Robotics*, vol. 23, no. 4, pp. 625-649, Aug. 2007

[7] D. Zhang, "Parallel Robotic Machine Tools, Springer" *Science & Business Media*, Springer, London 2010

[8] M. C. Kim *et al*., "Remotely Manipulated Peg-in-Hole Task Conducted by Cable-Driven Parallel Robots," in *IEEE/ASME Transactions on Mechatronics*, vol. 27, no. 5, pp. 3953-3963, Oct. 2022

[9] M. Y. Cao *et al*., "Six-Axis Force/Torque Sensors for Robotics Applications: A Review," in *IEEE Sensors Journal*, vol. 21, no. 24, pp. 27238-27251, 15 Dec. 15, 2021

[10] J. Li *et al*., "A Compact FBG-Based Triaxial Force Sensor with Parallel Helical Beams for Robotic-Assisted Surgery," in *IEEE Transactions on Instrumentation and Measurement*, vol. 71, pp. 1-9, 2022

[11] R. M. Dreizler *et al*., "Theoretical Mechanics: Theoretical Physics 1", *Springer Science & Business Media,* 2010

[12] C. B. Black *et al*., "Parallel Continuum Robots: Modeling, Analysis, and Actuation-Based Force Sensing," in *IEEE Transactions on Robotics*, vol. 34, no. 1, pp. 29-47, Feb. 2018

[13] L. Lindenroth et al., "Intrinsic Force Sensing for Motion Estimation in a Parallel, Fluidic Soft Robot for Endoluminal Interventions," in *IEEE Robotics and Automation Letters*, vol. 7, no. 4, pp. 10581-10588, 2022

[14] Q. Liang *et al*., "Six-DOF Micro-manipulator Based on Compliant parallel Mechanism with Integrated Force Sensor", *Robotics and Computer-Integrated Manufacturing*, vol. 27, pp. 124-134, 2011

[15] C. Chen *et al*., "Stable Motion Control Scheme Based on Foot-Force Distribution for a Large-Scale Hexapod Robot," *2019 IEEE 4th International Conference on Advanced Robotics and Mechatronics (ICARM)*, Toyonaka, Japan, 2019, pp. 763-768

[16] Z. J. Wang *et al*., "Optimal Design and Experiment Research of a Fully Pre-stressed Six-axis Force/torque Sensor", *Measurement*, vol. 46, pp. 2013-2021, 2013

[17] Y.H. Wang *et al*., "Interaction Force Measurement of Parallel Robots Based on Structure-integrated Force Sensors Using Interpretable Linear Neural Networks." *Mechatronics*, vol. 87, 2022

[18] J-P. Merlet *et al*., "Solving the Forward Kinematics of a Gough-type Parallel Manipulator with Interval Analysis." *The International Journal of Robotics Research*, vol. 23, no. 3, pp. 221-235, 2004

[19] J. K. Xue *et al*., "A Novel Swarm Intelligence Optimization Approach: Sparrow Search Algorithm." *Systems science & control engineering* , vol. 8 no. 1 pp. 22-34, 2020

[20] G. Farhad, *et al.* "Advances in Sparrow Search Algorithm: a Comprehensive Survey." *Archives of Computational Methods in Engineering*, vol. 30 no. pp. 427-455, 2023